

# Chapter 16

## The Impact of Energetic Particle Precipitation on the Chemical Composition of the Middle Atmosphere: Measurements and Model Predictions

Miriam Sinnhuber, Nadine Wieters, and Holger Winkler

**Abstract** We investigate the impact of energetic particle precipitation on the chemical composition of the middle atmosphere by developing models, and combining model results with observations of the chemical response to particle precipitation events. We show that in the upper stratosphere and lower mesosphere, negative ion chemistry plays a role in addition to the well-known NO<sub>x</sub> and HO<sub>x</sub> production due to positive ion chemistry, releasing chlorine from its reservoir, and re-partitioning NO<sub>y</sub>. Model results also show a large direct impact of energetic electron precipitation on the chemical composition of the upper stratosphere and mesosphere, both during large solar events and during and after geomagnetic storms. Observations show that the indirect impact of energetic electron precipitation events on the middle atmosphere composition can be much larger than the impact of even large solar particle events. However, observations have not shown clear evidence for a direct impact of energetic electron precipitation at altitudes below 80 km so far; if there is a direct impact of energetic electron precipitation on the lower mesosphere and upper stratosphere as suggested by the model results, then it is small compared to the direct contribution of large solar events, or to the indirect impact of energetic electron precipitation due to downward propagation of mesospheric or thermospheric air during polar winter.

---

M. Sinnhuber · N. Wieters · H. Winkler  
Institute of Environmental Physics, University of Bremen, Otto-Hahn Allee. 1, 28359 Bremen,  
Germany

N. Wieters  
e-mail: [nwieters@iup.physik.uni-bremen.de](mailto:nwieters@iup.physik.uni-bremen.de)

H. Winkler  
e-mail: [hwinkler@iup.physik.uni-bremen.de](mailto:hwinkler@iup.physik.uni-bremen.de)

M. Sinnhuber (✉)  
Institute for Meteorology and Climate Research, Karlsruhe Institute of Technology, Hermann-von  
Helmholtz Platz. 1, 76344 Leopoldshafen, Germany  
e-mail: [miriam.sinnhuber@kit.edu](mailto:miriam.sinnhuber@kit.edu)

## 16.1 Introduction: Energetic Particle Precipitation

Energetic particles that precipitate into the Earth's atmosphere come from different sources which display different relations to the 11-year solar cycle depending on how particle flux and spectrum are modulated by solar activity.

High-energy particles, mainly protons of 1 MeV to several 100 MeV that can precipitate into the upper stratosphere, are associated with solar coronal mass ejections or solar flares which occur mainly around the solar maximum. These are called *Solar Proton Events* or *Solar Particle Events* (SPEs) as they are associated with an increase of proton fluxes of several orders of magnitude as measured by particle counters onboard geostationary satellites. As the terrestrial atmosphere is shielded against charged particles by its magnetic field, solar particles can precipitate into the Earth's atmosphere only in the region of the polar caps, the area typically  $>60^\circ$  geomagnetic latitude.

*Galactic cosmic rays* (GCRs) are particles of even higher energies which precipitate into the troposphere everywhere. They originate from outside the solar system and provide a continuous particle flux that is moderated by the varying strength of the solar magnetic field throughout the solar cycle.

Solar wind particles can be coupled into the terrestrial geomagnetic field in the magnetotail. There they can either be accelerated into the interior field, forming the source of auroral particles, or be trapped in the magnetosphere, forming the radiation belts. Auroral particles, mainly electrons with energies up to 10 keV, precipitate into the lower thermosphere ( $\geq 90$  km) in the auroral oval, at the inner boundary of the polar caps ( $\approx 65^\circ$  geomagnetic latitude). Particles trapped in the radiation belts can be accelerated during *geomagnetic storms* to energies ranging from tens of keV to several MeV, and precipitate into the atmosphere in so-called *Energetic Electron Precipitation* (EEP) events. These particles precipitate into the atmosphere in geomagnetic latitudes connecting to the radiation belts ( $\approx 59^\circ$ – $68^\circ$  geomagnetic latitude [Horne et al., 2009]). Geomagnetic storms are initiated by disturbances in the interplanetary plasma, which can be due to, e.g., fast solar wind streams or solar coronal mass ejections. They can occur in all phases of the solar cycle but are more frequent during solar maximum and in the transition from solar maximum to solar minimum, and more rare during the deep solar minimum.

*Energetic Particle Precipitation* (EPP) into the atmosphere leads to decomposition and ionization of the most abundant species ( $\text{N}_2$ ,  $\text{O}_2$ ,  $\text{H}_2\text{O}$ , O, or NO, depending on altitude). Ionization of the atmosphere leads to fast ion chemistry in which large cluster ions are formed from the primary  $\text{O}^+$ ,  $\text{O}_2^+$ ,  $\text{N}_2^+$  and  $\text{NO}^+$  ions, and chemically relatively inert  $\text{H}_2\text{O}$  and  $\text{N}_2$  are transformed into the chemically active radicals H, OH [Swider and Keneshea, 1973; Solomon et al., 1981], N, NO [Crutzen et al., 1975; Porter et al., 1976; Rusch et al., 1981] and O [Porter et al., 1976]. Both HOx (H, OH,  $\text{HO}_2$ ) and NOx (N, NO,  $\text{NO}_2$ ) can destroy ozone in catalytic cycles, HOx mainly at altitudes above 45 km, NOx more effectively at altitudes below 45 km [Lary, 1997].

Both excess NOx and ozone loss have been observed during and after large solar proton events, and are reproduced by chemical models reasonably well, e.g.,

[Solomon *et al.*, 1983; Jackman *et al.*, 2001, 2005b; Rohen *et al.*, 2005]. While HO<sub>x</sub> is short-lived, and HO<sub>x</sub> recovers quickly after the event, NO<sub>x</sub> can be very long-lived in the polar middle atmosphere especially during polar winter, when it can also be transported down into the stratosphere and destroy ozone there [Sinnhuber *et al.*, 2003b; Jackman *et al.*, 2005a; Winkler *et al.*, 2008]. This is called the *indirect effect* of particle precipitation. Enhanced NO<sub>x</sub> values have indeed been observed in the mid-stratosphere after the July 2000 solar proton event [Randall *et al.*, 2001]. These observations can be explained by downward propagation of particle-induced NO<sub>x</sub>, and are quite well reproduced by chemistry-transport models of the middle atmosphere, e.g., [Sinnhuber *et al.*, 2003c]. Thus, the impact of large SPEs on NO<sub>x</sub> and ozone loss seems to be qualitatively well understood, but not much is known about the impact of atmospheric ionization on other trace gases besides NO<sub>x</sub> and ozone.

The impact of energetic electron precipitation directly into the middle atmosphere is not as well investigated as that of the large solar particle events. It has been emphasized by some authors that EEPs can have a similar large impact on the chemical composition of the mesosphere and stratosphere as SPEs [Callis *et al.*, 1998; Siskind and Russel III, 1996; Siskind *et al.*, 2000]. Measurements of ozone in high polar latitudes suggest a large influence of magnetospheric electrons of relativistic energies on ozone concentrations in the mid-stratosphere winter [Sinnhuber *et al.*, 2006]. However, observations of the *direct effect* of energetic electron precipitation during an EEP—i.e., the local production of NO<sub>x</sub> and HO<sub>x</sub>, and subsequent ozone loss during the particle event—have been shown to be more complicated than for SPEs, possibly because the magnetospheric electrons precipitate into a much smaller area. In recent years, direct observations of large NO<sub>x</sub> productions due to EEPs have been reported two times [Renard *et al.*, 2006; Clilverd *et al.*, 2009]. These, however, have been interpreted by other authors as downward propagation of NO<sub>x</sub> from the upper mesosphere or lower thermosphere, probably produced by auroral precipitation [López-Puertas *et al.*, 2006; Funke *et al.*, 2007]. Enhanced OH values have been reported to be correlated with geomagnetic storms in a recent paper by Verronen *et al.* [2011]. However, in this case, significant enhancements were observed only above 70 km, and it is, to date, not clear whether energetic electrons can directly impact the stratosphere and lower mesosphere.

Thus, it seems that the NO<sub>x</sub> production and subsequent ozone loss during large solar events are reasonably well understood. However, two questions are still open:

- Are other constituents besides NO<sub>x</sub> and ozone affected by atmospheric ionization, and if yes, by how much?
- How does the impact of EEPs compare to that of SPEs, i.e. is the impact on the chemical composition of the middle atmosphere and particularly on stratospheric ozone comparable to that of large solar events?

These two questions will be addressed in the following using a combination of models of different complexity with observations of middle atmosphere constituents during and after large particle precipitation events.

In Sect. 16.2, the models used for the investigation are described. Section 16.3 describes the Heppa model versus MIPAS data intercomparison initiative, a multi-model intercomparison of chemical changes during and after the October/November

2003 solar particle event, and discusses the most important results of this initiative. In Sect. 16.4, the impact of negative ions on the atmospheric composition is discussed using results from the UBIC ion chemistry model; in Sect. 16.5, the impact of energetic electron precipitation is investigated.

Energetic particle precipitation impacts on the middle atmosphere are also discussed in Chaps. 8, 9, 15, and 17.

## 16.2 Models

We use models of different complexity to address different aspects of the chemical changes and dynamical couplings related to energetic particle precipitation, ranging from the one-dimensional box-model of middle atmosphere ion chemistry (UBIC, Sect. 16.2.3) to global models of chemistry and transport in the middle atmosphere either driven by prescribed temperatures and wind-fields (B3dCTM, Sect. 16.2.2) or free-running (B2dM, Sect. 16.2.1).

The neutral models share the same description of chemistry, which is based on the SLIMCAT chemistry code [Chipperfield, 1999]. This considers 58 neutral trace gases and about 180 gas phase, photochemical, and heterogeneous reactions between those trace species. Reaction rates and absorption cross sections are prescribed by the JPL recommendation of Sander *et al.* [2006].

Atmospheric ionization due to energetic particle precipitation is provided by the AIMOS model, which calculates global altitude-dependent three-dimensional distributions of atmospheric ionization based on observed proton and electron fluxes [Wissing and Kallenrode, 2009], see also Chap. 13. The impact of positive ion chemistry and particle induced decomposition of  $N_2$  and  $O_2$  is parameterized based on Rusch *et al.* [1981]; Porter *et al.* [1976] and Solomon *et al.* [1981]. Hence 1.25 NO<sub>x</sub> are produced (of which 45 % are N, and 55 % NO) as well as up to 2 HO<sub>x</sub> constituents depending on altitude and ionization rate, and 1.15 O per ion pair.

### 16.2.1 The Bremen 2-Dimensional Model B2dM

The Bremen 2-dimensional model (B2dM) has been developed originally as a combination of the THIN AIR 2-dimensional general circulation model [Kinnersley, 1996] and the chemistry code of the SLIMCAT model [Chipperfield, 1999]. The model calculates temperature, pressure and wind fields on isentropic surfaces driven by prescribed sea-surface temperatures and the Montgomery potential. The vertical extent in its present setting is from the surface to about 100 km with a vertical spacing of about 3 km; the horizontal resolution is rather poor, with 19 grid boxes equally distributed in latitude from pole to pole (about 9°). The model uses a family approach considering Ox ( $O_3 + O(^3P) + O(^1D)$ ), NO<sub>x</sub> (N + NO + NO<sub>2</sub>), ClO<sub>x</sub> (Cl + ClO + 2Cl<sub>2</sub>O<sub>2</sub>), BrO<sub>x</sub> (Br + BrO), HO<sub>x</sub> (H + OH + HO<sub>2</sub>), and CHO<sub>x</sub>

(CH<sub>3</sub>, CH<sub>3</sub>O<sub>2</sub>, CH<sub>3</sub>OOH, CH<sub>3</sub>O, CH<sub>2</sub>O and HCO) in the stratosphere, and a non-family version using exactly the same reactions and rates in the mesosphere above ≈55 km. The Bremen 2-dimensional model has been used in a number of studies to investigate the impact of energetic particle precipitation on the middle atmosphere in the past [Sinnhuber *et al.*, 2003b, 2003c; Rohen *et al.*, 2005; Winkler *et al.*, 2008].

### 16.2.2 *The Bremen 3-Dimensional Chemistry and Transport Model B3dCTM*

The Bremen 3-dimensional Chemistry and Transport Model (B3dCTM) is a combination of the chemistry-transport model CTM-B [Sinnhuber *et al.*, 2003a] with the chemistry code of the Bremen 2-dimensional model of the stratosphere and mesosphere [Sinnhuber *et al.*, 2003b; Winkler *et al.*, 2008]. The B3dCTM is a global 3-dimensional model with a horizontal resolution of 3.75° in longitude and 2.5° in latitude, which is forced by prescribed temperatures and wind-fields, thus, the vertical range of this model is restricted by the availability of these data. Advection is calculated by using the second order moments scheme of Prather [1986]. Two versions of this model have been used in this investigation:

The first version of the model uses isentropic surfaces. The lower model boundary is limited by the use of potential temperature as vertical coordinate. Vertical transport perpendicular to the isentropes is derived from diabatic heating and cooling rates calculated using the MIDRAD radiation scheme [Shine, 1987]. This will be called the *stratospheric* model version in the following. Here results from model runs driven by European Centre for Medium-Range Weather Forecasts (ECMWF) (ERA Interim [Simmons *et al.*, 2006; Dee *et al.*, 2011]) reanalysis are used, which restricts the model upper boundary to 0.1 hPa (55–60 km), with a vertical resolution of about 1 km in the lower stratosphere, increasing to about 4 km at 60 km altitude.

Additionally, a model version has been developed which runs on isobaric surfaces; this enables us to extend the vertical range of the model based on the availability of meteorological data. At the moment, data from the LIMA general circulation model [Berger, 2008] are used, which is nudged to ECMWF ERA 40 in the lower stratosphere, and covers the vertical range from the surface to ≈130–140 km. This will be called the *LIMA* model version in the following; it currently runs on 30 isobaric surfaces from 247.8 to 0.00016 hPa (approximately 10 to 100 km) with a vertical resolution of approximately 3 km. The transport is calculated by vertical and horizontal wind fields as provided by the LIMA model.

Both model versions use the same family chemistry scheme as the 2-dimensional model in the stratosphere (Sect. 16.2.1); however, a non-family version for the mesospheric chemistry has been developed for the LIMA model version. Both model versions use a parameterization for NO<sub>x</sub> and HO<sub>x</sub> production due to positive ion chemistry as discussed above; additionally, parameterizations for negative ion chemistry developed based on results from the UBIC model (Sect. 16.2.3) can be used (see Sect. 16.4, Fig. 16.5). Results from the same model family based on CTM-B are

**Table 16.1** Positive ions, negative ions, and neutral species implemented in the UBIC model

Cations	$N^+$ , $N_2^+$ , $NO^+$ , $NO_2^+$ , $O^+(^4S)$ , $O^+(^2D)$ , $O^+(^2P)$ , $O_2^+$ , $O_2^+(a^4)$ , $O_4^+$ , $O_5^+$ , $H^+$ , $CO^+$ , $CO_2^+$ , $HCO^+$ , $H_2O^+$ , $O_2^+(H_2O)$ , $H^+(H_2O)_{n=1...7}$ , $H^+(H_2O)(OH)$ , $H^+(H_2O)(CO_2)$ , $H^+(H_2O)_2(CO_2)$ , $H^+(H_2O)(N_2)$ , $H^+(H_2O)_2(N_2)$ , $H^+(CH_3CN)$ , $H^+(CH_3CN)(H_2O)_{n=1...6}$ , $H^+(CH_3CN)_2$ , $H^+(CH_3CN)_2(H_2O)_{n=1...4}$ , $H^+(CH_3CN)_3$ , $H^+(CH_3CN)_3(H_2O)_{n=1,2}$ , $NO^+(H_2O)$ , $NO^+(H_2O)_2$ , $NO^+(H_2O)_3$ , $NO^+(CO_2)$ , $NO^+(N_2)$ , $NO^+(H_2O)(CO_2)$ , $NO^+(H_2O)_2(CO_2)$ , $NO^+(H_2O)(N_2)$ , $NO^+(H_2O)_2(N_2)$ , $NO_2^+(H_2O)_{n=1,2}$
Anions	$e^-$ , $O^-$ , $O_2^-$ , $O_3^-$ , $O_4^-$ , $OH^-$ , $NO_2^-$ , $NO_3^-$ , $CO_3^-$ , $CO_4^-$ , $CH_3^-$ , $HCO_3^-$ , $O^-(H_2O)$ , $O_2^-(H_2O)_{n=1,2}$ , $O_3^-(H_2O)_{n=1,2}$ , $OH^-(H_2O)_{n=1,2}$ , $NO_2^-(H_2O)_{n=1,2}$ , $NO_3^-(H_2O)_{n=1,2}$ , $CO_3^-(H_2O)_{n=1,2}$ , $NO_3^-(HNO_3)_{n=1...4}$ , $NO_3^-(HNO_3)(H_2O)$ , $NO_3^-(HNO_3)_2(H_2O)$ , $H_2SO_4^-$ , $HSO_4^-(H_2SO_4)_{n=1,2}$ , $HSO_4^-(H_2SO_4)(H_2O)$ , $HSO_4^-(HNO_3)_{n=1,2}$ , $HSO_4^-(HNO_3)(H_2O)$ , $HSO_4^-(HNO_3)_2(H_2O)$ , $HSO_4^-(H_2SO_4)(HNO_3)$ , $HSO_4^-(H_2SO_4)(HNO_3)(H_2O)$ , $Cl^-$ , $Cl_2^-$ , $Cl_3^-$ , $ClO^-$ , $ClO^-(HCl)$ , $ClO^-(H_2O)$ , $ClO^-(CO_2)$ , $ClO^-(HO_2)$ , $NO_3^-(HCl)$
Neutrals	$N(^4S)$ , $N(^2D)$ , $N_2$ , $O(^3P)$ , $O(^1D)$ , $O_2$ , $O_3$ , $H$ , $H_2$ , $OH$ , $HO_2$ , $NO$ , $NO_2$ , $NO_3$ , $N_2O$ , $H_2O$ , $CH_4$ , $CH_3$ , $CO_2$ , $CO$ , $HCO_3$ , $HNO_3$ , $HNO_2$ , $N_2O_5$ , $H_2SO_4$ , $CH_3CN$ , $Cl$ , $Cl_2$ , $ClO$ , $CINO_2$ , $CIONO_2$ , $HCl$ , $HOCl$

also shown in Chap. 9. The B3dCTM is also used to investigate diurnal variations of ozone measured above Ny Ålesund, Spitsbergen, by a ground-based microwave instrument (see Chap. 8). The *B3dCTM LIMA* model version as well as the combination with UBIC parameterizations have been developed in the framework of the priority program CAWSES funded by the German funding agency *Deutsche Forschungsgemeinschaft* DFG.

### 16.2.3 The University of Bremen Ion Chemistry Model UBIC

The University of Bremen Ion Chemistry (UBIC) model [Winkler, 2007; Winkler et al., 2009] has been developed to study the ion chemistry of the middle atmosphere, and the interaction with neutral species in detail. In particular, it can be used to simulate the impact of energetic particle precipitation on middle atmosphere chemistry. UBIC is an ion chemistry box model which simulates the time evolution of 138 charged and uncharged species considering more than 600 reactions using the semi-implicit symmetric integration method [Ramarson, 1989]. Table 16.1 lists all charged and neutral species considered in UBIC. The model accounts for photo-ionization of NO by Lyman- $\alpha$  radiation, as well as photo-dissociation and photo-detachment of electrons. Particle impact ionizations are considered by the means of external ionization rates, e.g. provided by the AIMOS model [Wissing and Kallenrode, 2009], see also Chap. 13.2; additionally, a parameterization for Galactic cosmic rays is implemented [Heaps, 1978]. The ionization is distributed on the main atmospheric constituents  $N_2$  and  $O_2$  according to their abundance and ionization cross sections [Rusch et al., 1981; Porter et al., 1976; Zipf et al., 1980]. The model's

set of reactions is a combination of the reactions assumed to govern the ion chemistry in the stratosphere, mesosphere, and lower thermosphere, taken from *Brasseur and Chatel* [1983]; *Viggiano et al.* [1994]; *Kopp* [1996]; *Rees* [1998]; *Kazil* [2002]; *Verronen* [2006]. UBIC can either be used on-line with a neutral chemistry model or it can operate as an equilibrium model to calculate plasma concentrations and production rates of uncharged species due to ionizations. UBIC is also used to calculate parameterizations of ion chemistry impacts on the neutral atmosphere for the use in global models (see Sect. 16.4). UBIC has been developed within CAWSES based on an older model version considering only a simple positive ion scheme to investigate in detail the impact of ion chemistry on atmospheric composition during large energetic particle events (see, e.g., Sect. 16.4).

### 16.3 The Heppa Model Versus MIPAS Data Intercomparison Study

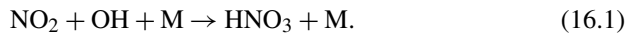
On October 29, 2003, one of the largest solar proton events recorded so far occurred. This event was exceptional both for its size, and for the fact that it was covered very well by global observations from several satellite instruments detecting both the expected NO<sub>x</sub> increase [*Jackman et al.*, 2005a; *López-Puertas et al.*, 2005a] and ozone loss [*Jackman et al.*, 2005a; *Rohen et al.*, 2005]. Additionally, MIPAS/ENVISAT observed a number of trace species that have not been observed during an SPE before, e.g., HNO<sub>3</sub>, N<sub>2</sub>O<sub>5</sub>, ClONO<sub>2</sub>, HOCl, ClO, and others [*López-Puertas et al.*, 2005b; *von Clarmann et al.*, 2005]. These observations provided a unique natural experiment to test our understanding of the chemical changes during and after large atmospheric ionization events.

A model-measurement intercomparison study was set up involving nine models of different complexity including a 1D/2D model, 3-dimensional global chemistry-transport models, and 3-dimensional global coupled chemistry-climate models, the so-called *Heppa model versus MIPAS data intercomparison study*, or *Heppa intercomparison*, [*Funke et al.*, 2011]. All nine models carried out model experiments for the time-period of the October/November 2003 SPE using the same set of ionization rates considering both protons and electrons provided by the AIMOS model (*Wissing and Kallenrode* [2009], see also Chap. 13). Model results of temperature, CH<sub>4</sub>, CO, NO, NO<sub>2</sub>, N<sub>2</sub>O, HNO<sub>3</sub>, N<sub>2</sub>O<sub>5</sub>, HNO<sub>4</sub>, O<sub>3</sub>, H<sub>2</sub>O<sub>2</sub>, ClO, HOCl, and ClONO<sub>2</sub> were provided on the geolocation and local time of MIPAS overpass, and compared against the MIPAS observations. Both the B2dM and the B3dCTM participated in the Heppa intercomparison study (see *Funke et al.* [2011]). B3dCTM provided hourly model output. As B2dM considers a zonally averaged state, and thus cannot consider longitudinal inhomogeneity of the polar cap which is a result of the displacement of the geomagnetic pole to the geographic pole, model runs were carried out for different longitudes with B2dM. 1-dimensional model runs were initialized from these B2dM model runs at the positions of individual MIPAS measurements, and model results were thus provided at the local time and geolocation of every individual MIPAS observation.

Results from the Heppa intercomparison initiative considering results from all nine contributing models have been published recently (see *Funke et al.* [2011]). Here we will give an overview of the most important results concerning our understanding of processes during and after particle precipitation events. Results from the Heppa initiative are also given in Chap. 15.

In the multi-model average, there is good agreement with observed changes both for NO<sub>y</sub> production and ozone loss during the event at most altitudes (see Fig. 15.9 in Chap. 15 for NO<sub>y</sub> changes). Systematic differences between MIPAS measurements and model results are observed around 1 hPa, where NO<sub>y</sub> is overestimated by all models, and above 0.2 hPa, where NO<sub>y</sub> production is underestimated by all models compared to the observations; this may be due to systematic features in the ionization rates. However, there is also a very large variability and spread between models, and between individual models and the observations. This variability is apparently related to the different dynamics of the participating models, especially to the vortex strength and stability, which varies greatly from model to model. Results of the intercomparison of NO<sub>y</sub> are also discussed in more detail in Chap. 15.

During the October/November 2003 SPE, an increase of HNO<sub>3</sub> was observed for the first time as a response to a large atmospheric ionization event. The increasing NO<sub>x</sub> and HO<sub>x</sub> concentrations after an energetic particle precipitation event can lead to formation of nitric acid through the gas phase reaction



However, comparison of model results with MIPAS measurements show that the observed HNO<sub>3</sub> increase cannot be explained by neutral reactions due to the NO<sub>x</sub> and HO<sub>x</sub> increase alone as shown in Fig. 16.1 exemplarily for B2dM and B3dCTM. Two additional pathways have been proposed to explain the HNO<sub>3</sub> increase due to atmospheric ionization, both including ion chemistry reactions: Conversion of N<sub>2</sub>O<sub>5</sub> to HNO<sub>3</sub> in reactions with positive ion clusters [*Boehringer et al.*, 1983], and HNO<sub>3</sub> production through recombination of positive water clusters with negative NO<sub>3</sub><sup>-</sup>-containing ions [*Verronen et al.*, 2008]. *Verronen et al.* [2008] have investigated these observations using the SIC ion chemistry model, and found that the HNO<sub>3</sub> increase observed during the event can be interpreted qualitatively by recombination reactions between water cluster ions and NO<sub>3</sub><sup>-</sup>-containing ions; however, the observed increase is overestimated by the model during polar night up to a factor of 2.5 depending on altitude. Similar results as shown in Fig. 16.1 have been obtained by all models not considering HNO<sub>3</sub> formation due to ion chemistry. However, two models did consider additional HNO<sub>3</sub> formation due to ion chemistry: the FinRose model uses a parameterization of HNO<sub>3</sub> production based on the reaction pathway described in *Verronen et al.* [2008] and overestimates the HNO<sub>3</sub> increase during the event by more than a factor of 4; and the KASIMA model uses a parameterization of the water cluster ion chain [*Boehringer et al.*, 1983], see also Chap. 15. KASIMA also underestimates the HNO<sub>3</sub> increase during the event, but has better agreement for the second HNO<sub>3</sub> enhancement in late November than the other models (see also *Funke et al.* [2011]). This comparison shows that to understand the observed changes to HNO<sub>3</sub>, ion chemistry has to be taken into account. Qualitatively, the ion



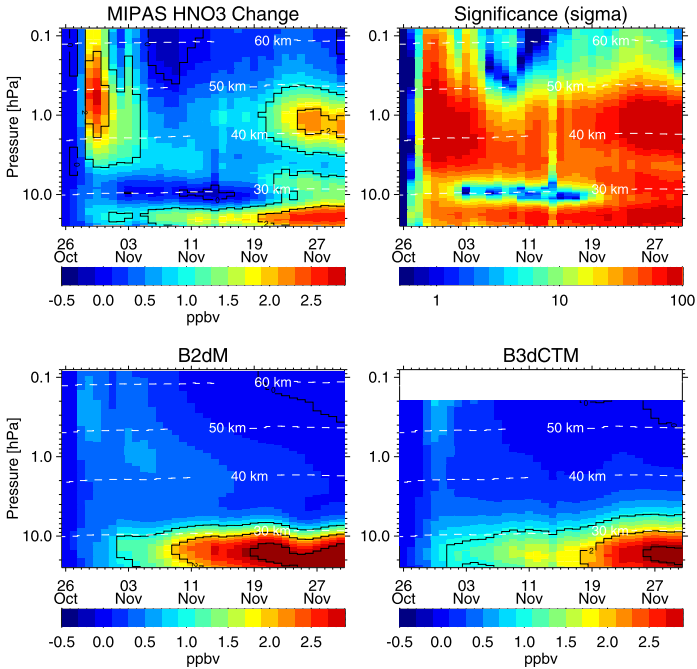


**Fig. 16.1** MIPAS  $\text{HNO}_3$  change averaged over  $70\text{--}90^\circ\text{N}$  during the October/November 2003 SPE, compared to modeled  $\text{HNO}_3$  changes by the B2dM and B3dCTM models using AIMOS ionization rates considering both protons and electrons, sampled at the geolocations and local times of the MIPAS observations. Also shown is the 1-sigma significance of the observations, the ratio of the average values to the standard deviation. Adapted from *Funke et al. [2011]*

chemistry processes appear to be understood, however, there are still problems to reproduce them quantitatively within the uncertainty of the observations.

Also observed for the first time during a large solar event were a number of chlorine species, namely  $\text{ClO}$ ,  $\text{HOCl}$ , and  $\text{ClONO}_2$ . Both  $\text{HOCl}$  and  $\text{ClONO}_2$  were found to increase during the SPE, while  $\text{ClO}$  increased at the vortex edge, but decreased in the vortex core. The decrease of  $\text{ClO}$  via the reaction  $\text{ClO} + \text{NO}_2$  is reproduced by the models qualitatively, but the absolute values are underestimated by about a factor of 2–4 as shown exemplarily for B2dM and B3dCTM in the left panel of Fig. 16.2; the increase of  $\text{ClO}$  at the vortex edge is not reproduced by the models, hinting at an additional chemical process not considered in the models (see *Funke et al. [2011]*). The increases of  $\text{HOCl}$  and  $\text{ClONO}_2$  were reproduced qualitatively by most models, however, the absolute values especially of  $\text{ClONO}_2$  were underestimated by most models (see also right panel of Fig. 16.2). This might be either due to an underestimation of  $\text{ClO}$  by the models already before the particle event (see *Funke et al. [2011]*), or to additional ion chemistry involving chlorine which is not included in the models. This latter possibility is investigated in more detail in the following Sect. 16.4.

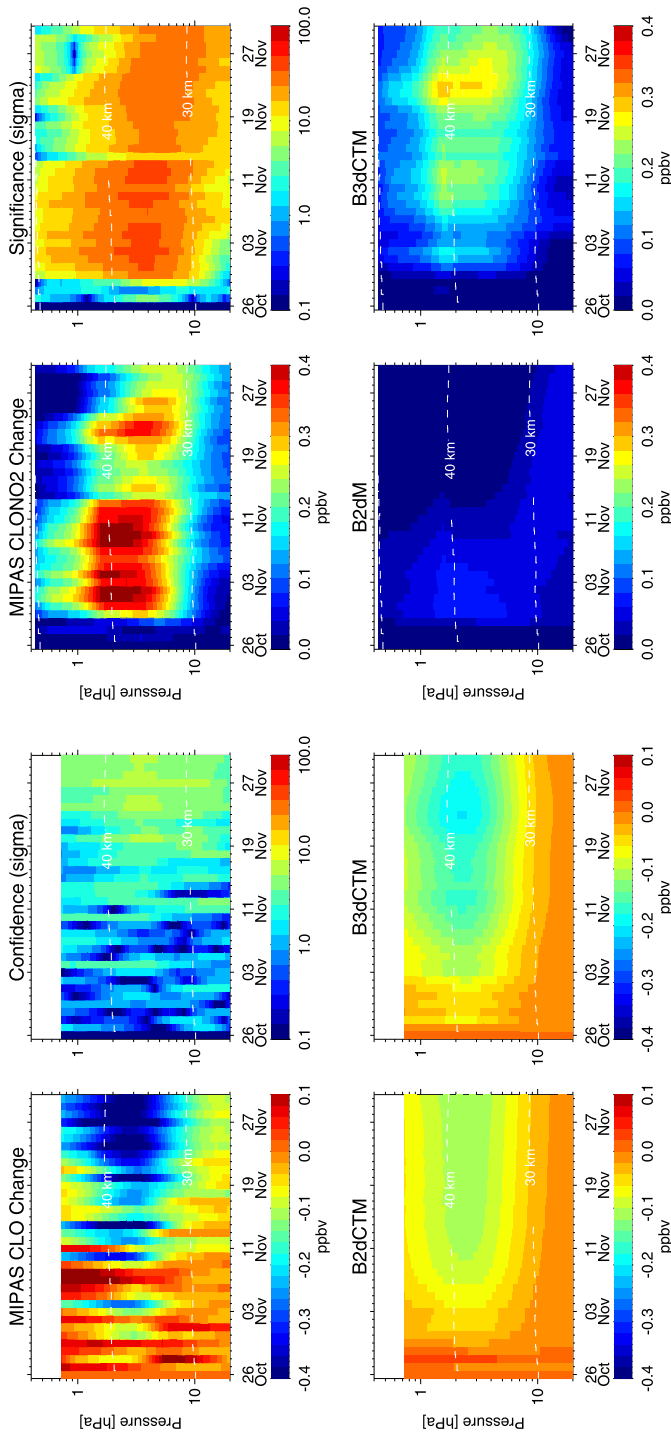


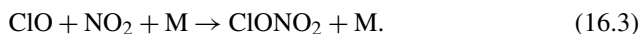
**Fig. 16.2** MIPAS CIO (*left*) and ClONO<sub>2</sub> (*right*) change averaged over 70–90°N during the October/November 2003 SPE, compared to modeled changes by B2dM and B3dCTM sampled to the MIPAS geolocations and local times. Also shown are the significances of the CIO and ClONO<sub>2</sub> observations (see Fig. 16.1). Right panel adapted from *Funke et al. [2011]*

## 16.4 The Role of Negative Ion Chemistry for Chlorine Activation During SPEs

The effects of solar particle events on NO<sub>x</sub> and ozone appear to be qualitatively well understood. They can be reproduced by atmospheric models considering the production of NO<sub>x</sub> and HO<sub>x</sub> parameterized as a result of positive ion chemistry. However, there have been considerable differences between model predictions and measurements concerning other chemical compounds, in particular nitrogen and chlorine species (see Sect. 16.3). It has been pointed out by *Solomon and Crutzen* [1981] that SPEs might influence chlorine chemistry due to the HO<sub>x</sub> and NO<sub>x</sub> increase by transforming hydrogen chloride into reactive chlorine:



followed by the formation of chlorine nitrate at the expense of reactive radicals, especially at stratospheric altitudes:

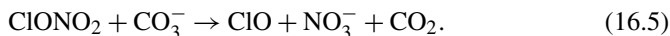


Model simulations which only account for NO<sub>x</sub> and HO<sub>x</sub> production due to positive ion chemistry fail to reproduce the observed chlorine perturbations (e.g. *Funke et al.* [2011], see also Sect. 16.3). Apparently, there are impacts on the neutral chemistry in addition to the well-known release of NO<sub>x</sub> and HO<sub>x</sub>. Therefore, a detailed consideration of the ion chemical processes is necessary to understand the chemical effects of EPPs. Here, we investigate the impact of negative ion chemistry on chlorine species in the upper stratosphere and lower mesosphere.

Under geomagnetically quiet conditions, negative chlorine species are a significant fraction of the total anion density in the mesosphere, see e.g. *Chakrabarty and Ganguly* [1989]; *Fritzenwallner and Kopp* [1998]. Therefore, it can be assumed that during EPPs reactions of negative ions influence the chlorine chemistry. Hydrogen chloride reacts with several anions to produce Cl<sup>-</sup>:



where X<sup>-</sup> can be {O<sub>2</sub><sup>-</sup>, O<sup>-</sup>, CO<sub>3</sub><sup>-</sup>, OH<sup>-</sup>, NO<sub>2</sub><sup>-</sup>, NO<sub>3</sub><sup>-</sup>}. The most abundant chlorine ions in the mesosphere are Cl<sup>-</sup> and Cl<sup>-</sup>(H<sub>2</sub>O), and while reactions of both species with atomic hydrogen re-release HCl, recombination reactions with cations can lead to a production of Cl, ClO, ClONO<sub>2</sub>, and Cl<sub>2</sub>, depending on the detailed reaction pathways. In the latter case, the reservoir compound HCl is partly converted to active chlorine species, similar as in reaction (16.2). Additionally, there is the reaction of chlorine nitrate with the carbon trioxide ion which is one of the most abundant anions in the lower mesosphere:



This reaction also transforms chlorine from a reservoir to a radical. Note that this process counteracts reaction (16.3). For further details on the atmospheric ion chemistry of chlorine see *Kopp* [1996]; *Kopp and Fritzenwallner* [1997].

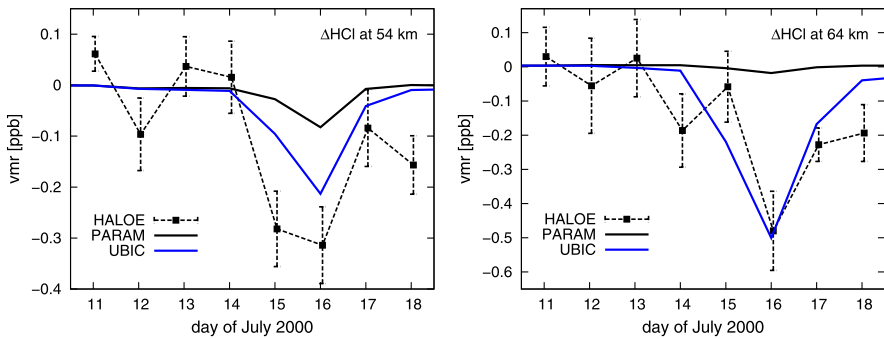


**Fig. 16.3** Differences of zonally averaged HCl mixing ratios during the solar proton event in July 2000 at two different altitudes for sunrise conditions (differences with respect to the mean HCl sunrise values of 10–12 July). Shown are HALOE data and simulation results from the atmospheric model at  $66.5^\circ$  North. The HALOE error bars represent one standard deviation. PARAM indicates the model with parametrized production rates for HOx and NOx, and UBIC the model with full ion chemistry. Figure adapted from *Winkler et al.* [2011]

In order to study the effect of the negative ion chemistry on chlorine species during an EPP event we have performed model simulations of the major SPE in July 2000, and compared them to HCl measurement data from the UARS HALOE instrument [*Russel et al.*, 1993]. The HALOE observations of HCl loss during the July 2000 SPE are also discussed in *Kazeminejad* [2009]. The results of the model study have been published in *Winkler et al.* [2009, 2011], and a brief summary is given here. For the purpose of our study, the 2-dimensional model B2dM was used (see Sect. 16.2.1) in combination with the UBIC ion chemistry model described in Sect. 16.2.3. Additional to the UBIC simulations, model runs with parameterized production of NOx and HOx due to the positive ion chemistry during the SPE have been carried out (assuming 1.25 NOx per ionization with 45 %  $N(^4S)$  and 55 %  $N(^2D)$  according to *Porter et al.* [1976]; *Rusch et al.* [1981], and up to two HOx constituents per ionization in the height region of interest according to *Solomon et al.* [1981]). These simulations are called PARAM model runs in the following. Figure 16.3 shows that the simulations with the UBIC model yield significantly larger HCl losses than the PARAM model runs, and they agree much better with the HALOE measurements. At  $\approx 64$  km altitude the HCl decrease predicted by the UBIC model for the main event phase (July 16) is in the order of 500 ppt (for sunrise conditions) which agrees with the HALOE observations of HCl decrease within error bars (actually, on this altitude and day the agreement is better than 4 %). The PARAM model is unable to reproduce the effect on HCl at that altitude. If all negative ion chemistry reactions involving chlorine species are switched off (not shown), the simulation results do not differ significantly from the PARAM results. Therefore, the differences arise from the negative ion chemistry of the chlorine species. At lower altitudes, the observed decrease of HCl mixing ratios is smaller and also the difference between the UBIC and PARAM results gets smaller. This is due to the fact that in the lower parts of the middle atmosphere the negative ion chemistry

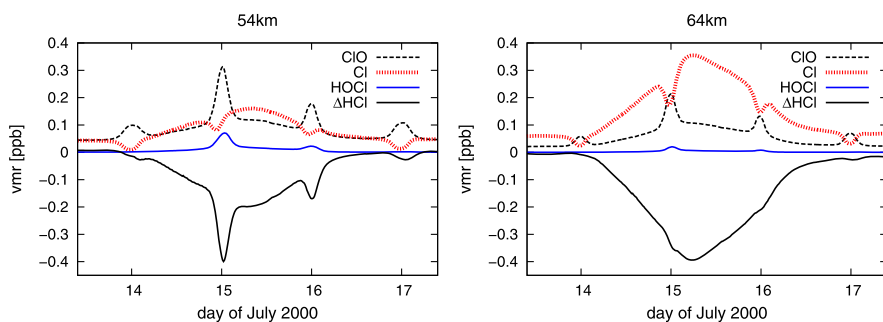


**Fig. 16.4** UBIC modeled  $\Delta\text{HCl}$  in comparison with other chlorine species during the solar proton event in July 2000 at 54 km and 64 km at  $66.5^\circ$  North. Figure adapted from *Winkler et al.* [2009]

is no longer dominated by chlorine species but rather by  $\text{HCO}_3^-$ ,  $\text{CO}_3^-$ ,  $\text{NO}_3^-$ , and their hydrates. The short-lived decrease of HCl during the SPE in July 2000 corresponds to increasing amounts of other chlorine species. Figure 16.4 shows the enhanced mixing ratios of Cl, ClO, and HOCl in comparison with the HCl loss; at these altitudes, all activated chlorine is transferred either to Cl, ClO, or HOCl, and the partitioning between the active chlorine species, and at 54 km also the amount of chlorine activated, depend on the solar zenith angle.

Systematic UBIC model runs have been performed to identify the key parameters on which the impacts on chlorine species depend. These parameters are: Ionization rate, solar zenith angle, pressure altitude, HCl, Cl + ClO, ClONO<sub>2</sub>, NO<sub>x</sub>, and H<sub>2</sub>O. From UBIC simulations considering these dependencies, a parameterization of the impact of the negative ion chemistry on chlorine activation and chlorine partitioning has been developed. The resulting lookup-table can be used by global three-dimensional models of the middle atmosphere to account for the chemical impact of negative ions on chlorine partitioning without running the time consuming ion chemistry model. This parameterization has been implemented in the *stratospheric* version of B3dCTM (see Sect. 16.2.2) to investigate the impact of negative chlorine chemistry on atmospheric composition during the large solar particle event of October/November 2003 on a global scale. First results are presented in Fig. 16.5. Given are the relative difference between model runs with and without ionization impacts, and the relative difference between model runs considering atmospheric ionization, with and without parameterization for negative chlorine ion chemistry. Generally speaking, the additional change of ClO, HOCl and ClONO<sub>2</sub> due to negative chlorine ion chemistry appears to be small compared to the chlorine activation due to the HO<sub>x</sub> increase at the latitudes, local times, and altitudes considered here. The largest changes—an increase of about 160 ppt—are observed for HOCl at altitudes above 40 km during the event. A small but significant decrease of ClONO<sub>2</sub> is observed during the event at altitudes around 40 km, and ClO also increases by about 80–100 ppt above 50 km during the event, leading to a maximal release of active chlorine of about 260 ppt above 50 km, comparable to the observed loss of HCl during the large SPE of July 2000 (see Fig. 16.3). This additional chlorine activation

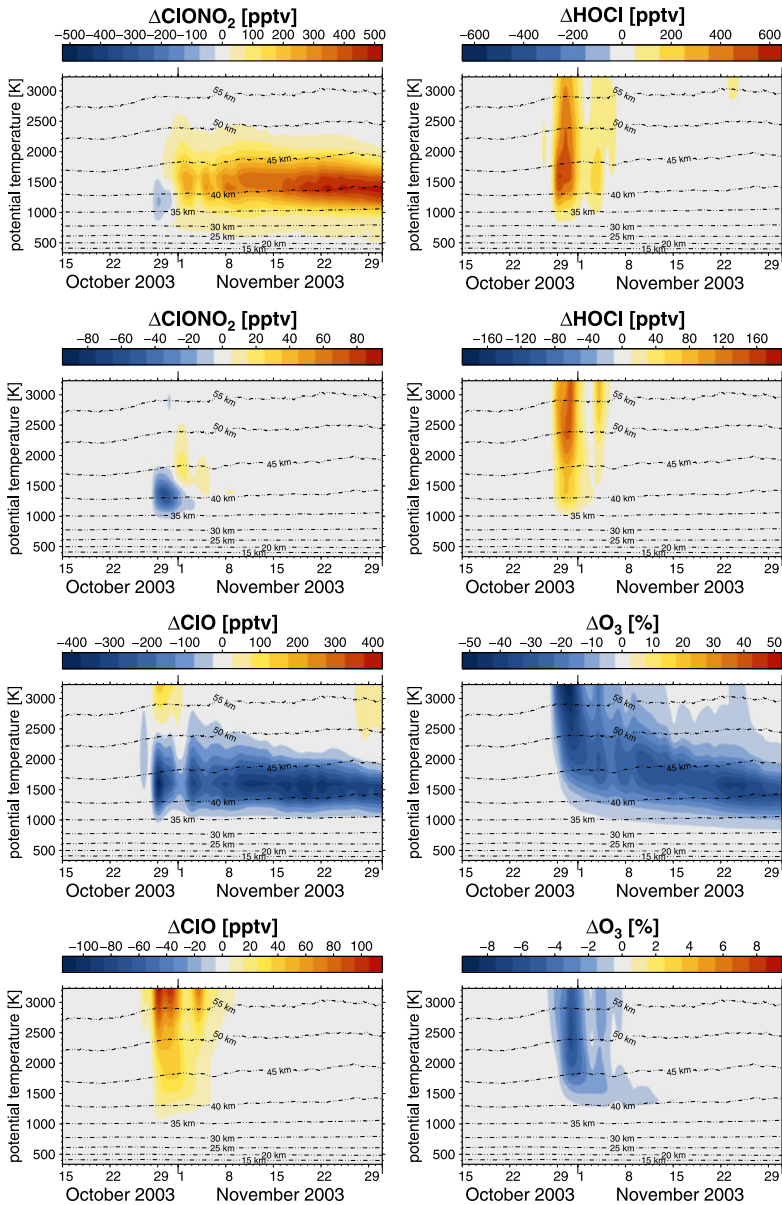


**Fig. 16.5** Impact of the SPE of October/November 2003 on chlorine species and ozone, northern polar cap mean values (70°N–90°N). Model results from the *stratospheric* version of B3dCTM using a parameterization of chlorine activation based on UBIC results. The *top* and *third* panel from the top show differences of the SPE model run considering HOx, NOx, and ClOy (UBIC parameterization) production and an undisturbed model run. The *second* panel from the top and the *lowest* panel show the differences due to the impacts of the negative chlorine chemistry (UBIC parameterization compared to the SPE run with HOx and NOx production only)

leads to additional ozone loss of several percent, with maximal values of up to 6 % during the event in an altitude range of 50–55 km.

## 16.5 The Role of Energetic Electron Precipitation

The potential impact of energetic electron precipitation into the atmosphere has been investigated in two ways: by carrying out model studies with the B3dCTM driven by AIMOS ionization rates with and without electron ionization, and by analyzing global observations of NO<sub>x</sub> on longer time-scales. Results from the first approach are discussed in Sect. 16.5.1, results from the second approach are discussed in Sect. 16.5.2.

### 16.5.1 Impact of Energetic Electrons on the Upper Stratosphere Based on Model Experiments

Model runs with the B3dCTM *stratosphere* version were carried out for the period October/November 2003 considering a ‘base’ situation without atmospheric ionization, a model scenario with atmospheric ionization considering protons only, and a model scenario considering atmospheric ionization by protons as well as electrons. Atmospheric ionization rates considering protons and electrons were provided by the AIMOS model (see Chap. 13). The period October/November 2003 was chosen because it contains a very large solar event on October 29/30, but also very high levels of geomagnetic activity before and after the solar event. Thus, both the additional impact of precipitating electrons during an SPE and the impact of electron precipitation during geomagnetic storms can be studied. Results from these model experiments have been published in *Wissing et al. [2010]*, see also Chap. 13.

In Fig. 16.6, results for a day of strong geomagnetic activity before the solar event are shown relative to the ‘base’ model run. Comparison of the model run with protons only and the model run with protons and electrons show significant ozone losses expected based on the AIMOS ionization rates from precipitating electrons above  $\approx 45$  km at high latitudes in both hemispheres, with maximum values of more than 15 % above 55 km.

In Fig. 16.7, NO<sub>x</sub> production during and after the large SPE are compared for model scenarios considering protons only, and considering protons and electrons. Considering electrons leads to larger NO<sub>x</sub> production both in Southern mid-latitudes, and in high polar regions in both hemispheres.

In Fig. 16.8, modeled ozone loss at the position of Ny Ålesund are shown considering protons and electrons, relative to a model run without atmospheric ionization. Here, results from the *LIMA* version of B3dCTM are shown, extending the altitude range to  $\approx 100$  km. Fairly significant ozone losses of more than 80 % are observed during the solar event, and areas of low ozone (losses of more than 10 % compared

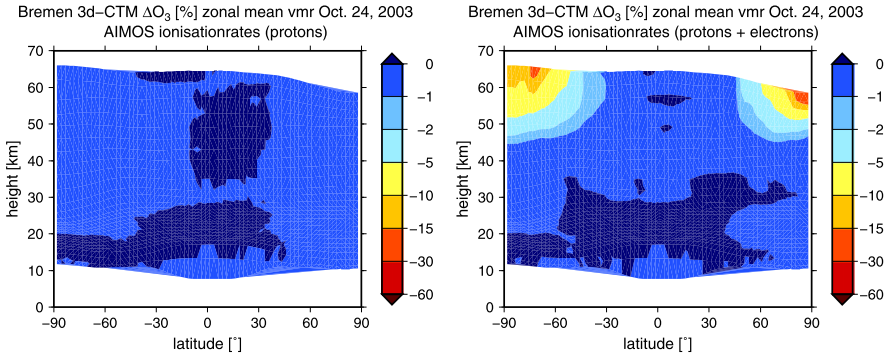


**Fig. 16.6** Modeled  $O_3$  changes due to atmospheric ionization using B3dCTM (stratospheric version) on a day of strong geomagnetic activity, considering protons only (left) and protons + electrons (right). Loss calculated relative to model run without atmospheric ionization. Adapted from *Wissing et al. [2010]*

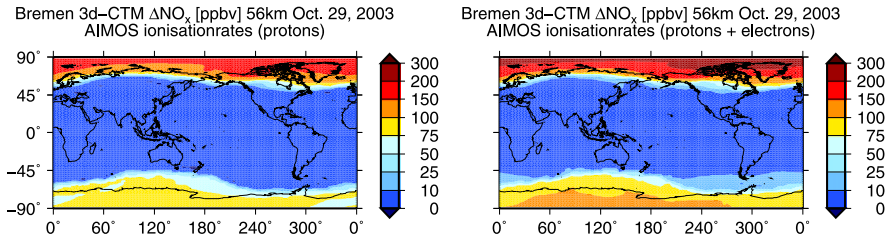


**Fig. 16.7** Modeled  $NO_x$  changes due to the October/November 2003 SPE using B3dCTM (stratospheric version), considering protons only (left) and protons + electrons (right). Loss and formation calculated relative to model run without SPE.  $NO_x$  formation globally on October 29 at 56 km. Adapted from *Wissing et al. [2010]*

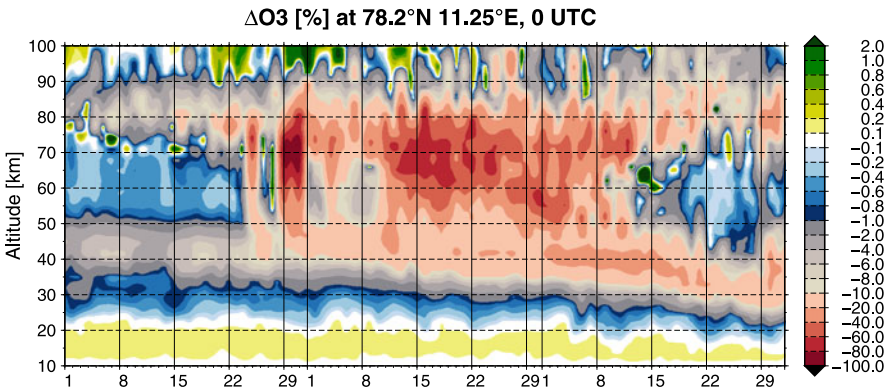


**Fig. 16.8** Ozone depletion due to atmospheric ionization in October and November 2003 around the large solar event of October/November 2003 as modeled by the *LIMA* version of B3dCTM considering both protons and electrons. Ozone changes relative to an undisturbed model run at a model box centered near Ny Ålesund



to the model run without ionization) propagate downward in the course of the following weeks. However, the strong electron event on October 24 already shown in Fig. 16.6 is also clearly visible. Significant ozone losses of 10–20 % are observed around October 24 at altitudes between  $\approx 50$ –80 km, and are transported down to 40 km altitude in the following days.

These model studies show that using ionization rates based on observed electron and proton fluxes, significant impacts of energetic electron precipitation are expected at altitudes below 60 km, both during large geomagnetic storms, and during and after large solar events. However, until now, no unambiguous observations have been published to show how realistic these model predictions are.

### 16.5.2 Impact of Energetic Electrons from Observations

Two data-sets of NO<sub>x</sub> (NO and NO<sub>2</sub>) observations from satellite-based instruments were used to investigate a possible impact of energetic electron precipitation on the middle atmosphere: HALOE/UARS [Russel *et al.*, 1993] and MIPAS/ENVISAT [Fischer *et al.*, 2008]. HALOE has been observing NO and NO<sub>2</sub> in an altitude range of 10–130 km from 1991 to the end of 2005 in solar occultation mode; MIPAS/ENVISAT was launched in 2002, and is expected to continue measurements until 2013. MIPAS observes NO and NO<sub>2</sub> in nominal limb mode in an altitude range from  $\approx 13$ –68 km. In this investigation, only measurements from October 2003 to March 2004 are used. As a solar occultation instrument, HALOE has a limited spatial resolution, taking 15 sun-rise and 15 sun-set observations in a very limited latitudinal range every day. However, HALOE data still present the longest continuous data-set of middle-atmosphere NO<sub>x</sub>. MIPAS has a much better spatial coverage than HALOE, but the time-series is yet not as long as the HALOE data-set, and also has been interrupted due to technical problems for nearly a year in 2004.

**HALOE/UARS** In Fig. 16.9, time-series of HALOE NO<sub>x</sub> in two different altitudes—60 and 80 km—are shown both for Northern and Southern high latitudes. Shown are daily averages poleward of 40° for both sun-rise and sun-set mode. At 60 km altitude, several solar particle events (July 2000 and October/November 2003) are clearly visible as large NO<sub>x</sub> enhancements; however, no clear response of NO<sub>x</sub> to energetic electron precipitation or geomagnetic storms is observed. However, a strong year-to-year variation of winter-time NO<sub>x</sub> is observed especially at 80 km, with highest values apparently during the transit from solar maximum to solar minimum (see also Kazeminejad [2009]). To investigate whether this interannual variation is due to energetic electron precipitation or geomagnetic activity, winter-time values of NO<sub>x</sub> (NDJF in the Northern hemisphere, MJJA in the Southern hemisphere) have been compared to the fluxes of energetic electrons both precipitating into the atmosphere from POES, and within the radiation belts from GOES, as well as with the Ap index, an indicator of geomagnetic activity, averaged over the same period of time. Both POES and GOES electrons are in the relativistic energy range

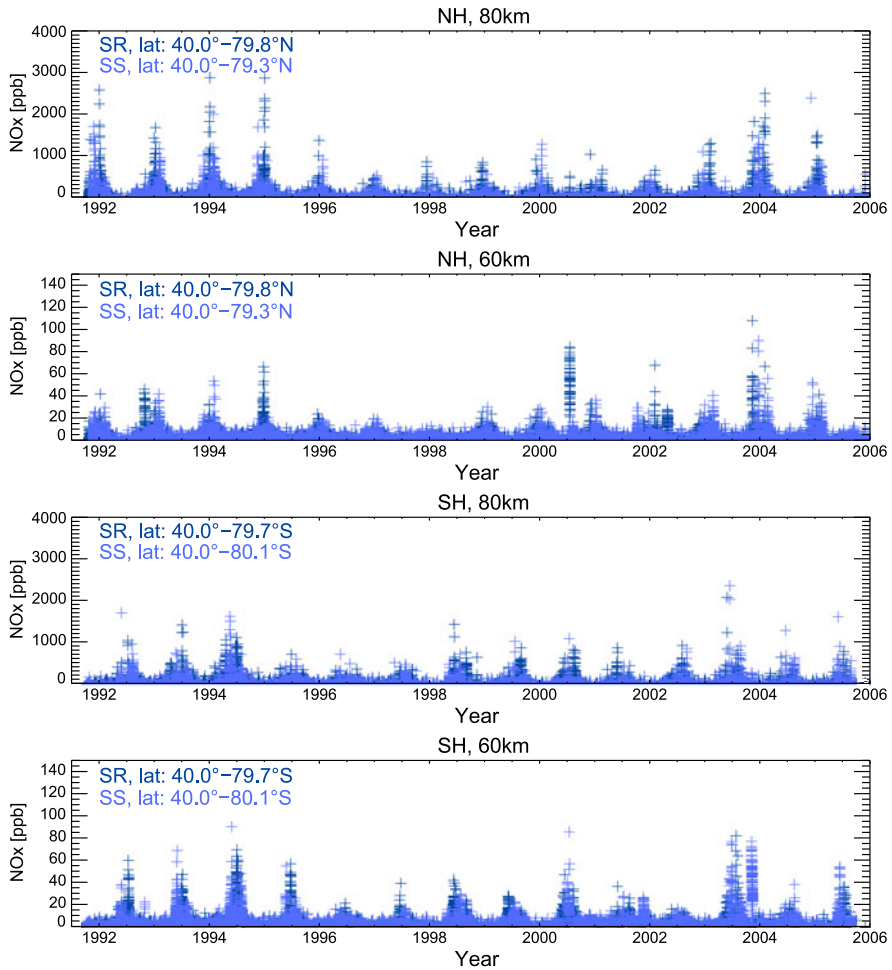


**Fig. 16.9** Time-series of daily averaged sun-rise and sun-set NOx ( $\text{NO} + \text{NO}_2$ ) as observed by HALOE/UARS. From *top* to *bottom*: 80 km in the Northern hemisphere; 60 km in the Northern hemisphere; 80 km in the Southern hemisphere; and 60 km in the Southern hemisphere. Figure adapted from *Kazeminejad [2009]*

(POES:  $>300$  keV, GOES:  $>2$  MeV) expected to precipitate into the lower mesosphere or even stratosphere.

Resulting correlation coefficients for both hemispheres are shown in Fig. 16.10 (see also *Kazeminejad [2009]*). Years with strong SPEs have been omitted here (2000 and 2003 in the Northern hemisphere, 2000 and 2005 in the Southern hemisphere). Error bars have been calculated as the result of a bootstrap method calculating correlation coefficients of 500 random permutations of the data-sets. A very high correlation is found between both geomagnetic activity and the fluxes of precipitating electrons (POES  $>300$  keV) in both hemispheres, with values with a statistical

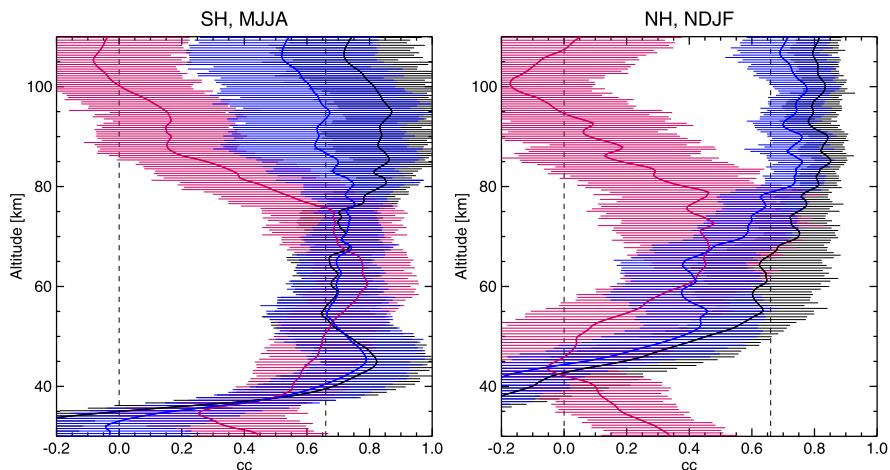


**Fig. 16.10** Correlation coefficients of HALOE NO<sub>x</sub> during polar winter (NDJF in the NH, MJJA in the SH) with Ap index (*black*), precipitating electrons of energies >300 keV as measured by POES (*blue*), and radiation belt electrons of >2 MeV as measured by GOES (*red*) averaged over the same time-period, for the Southern hemisphere (*left*) and the Northern hemisphere (*right*). Error bars are results from a bootstrap method. *Dashed vertical lines* mark a correlation coefficient of zero and 0.63, the latter referring to a significance of 1 % for a statistical ensemble of 14 data-points. Figure adapted from Kazeminejad [2009]

significance of better than 1 % at altitudes between  $\approx 40$ –100 km in the Southern hemisphere, and 70–130 km in the Northern hemisphere. A significant correlation is also found between radiation belt electrons (GOES >2 MeV) and NO<sub>x</sub> in the Southern hemisphere between  $\approx 60$ –80 km; in the Northern hemisphere, a positive correlation is found as well, but has a significance considerably lower than 1 %. The correlation of energetic electrons with NO<sub>x</sub> extends farther up into the atmosphere than expected from the energy range of the electrons especially for the POES electrons, probably because these electron fluxes are highly correlated to fluxes of electrons of lower energies, and also to geomagnetic activity. The correlation between radiation belt electrons and NO<sub>x</sub> is smaller than shown in Kazeminejad [2009] apparently because years with especially strong solar events have not been omitted there.

The observed correlation between NO<sub>x</sub> and geomagnetic activity respectively electron fluxes implies a significant impact of energetic electron precipitation on the composition of the middle atmosphere. However, it is not clear which altitudes are affected directly, as during winter-time, NO<sub>x</sub> will be transported downward in the polar vortex very efficiently. To investigate which altitudes are affected directly, summer-time values should be investigated. The annual variability of the correlation has been investigated further by Sinnhuber *et al.* [2011] in a project funded by the University of Bremen, and it was found that the direct impact of energetic electron precipitation and geomagnetic activity appears to be restricted to altitudes

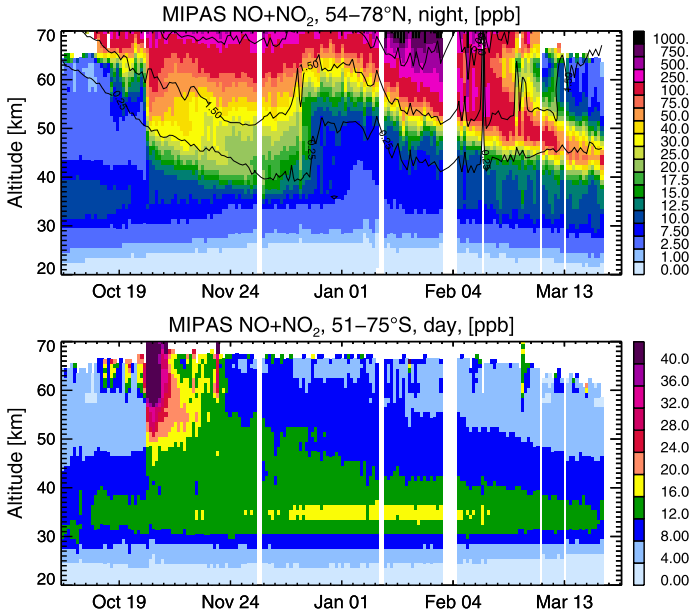


**Fig. 16.11** *Top*: MIPAS night-time NOx (NO + NO<sub>2</sub>) at high Northern latitudes (54–78°) from October 2003 to end of March 2004. *Solid lines* are the CO 0.25, 1.5, and 5.0 ppm isolines, an indicator for vertical motion within the polar vortex. Results for the Northern hemisphere are similar to those shown by López-Puertas *et al.* [2006]. *Bottom*: MIPAS day-time NOx at high Southern latitudes (51–75°S). MIPAS data courtesy B. Funke, Instituto de Astrofísica de Andalucía, and G. Stiller, KIT

above  $\approx 80$  km, while the impact of radiation belt electrons appears to be both less significant and not very robust.

**MIPAS/ENVISAT** In Fig. 16.11, daily averages of MIPAS NOx in the altitude range of 20–70 km are shown at high latitudes for both hemispheres from October 1, 2003 to March 31, 2004. This time-period was chosen because geomagnetic activity was very high throughout the complete time-series, and additionally, one of the strongest solar events occurred during this time in late October and early November. Also shown are isolines of CO, which is formed by photolysis of CO<sub>2</sub> in the upper mesosphere and thermosphere; as CO has a strong vertical gradient and is chemically inert during polar night, it can be used as a tracer of vertical motion in polar winter in conditions of low solar illumination. The impact of the large solar event is observed clearly in both hemispheres. In the Southern summer-time hemisphere, where the NOx lifetimes are short, this impact decreases continuously; in the Northern hemisphere, NOx values continue to stay high until December, when the signal is diluted quickly after a major stratospheric warming. The vortex reforms strongly after the warming, and a second NOx increase is observed in January and February in the Northern hemisphere which lasts until the end of the time-series in the upper stratosphere. This second NOx increase is likely due to transport from the upper

mesosphere or lower thermosphere as shown by the good correlation with CO isolines (see Fig. 16.11); no evidence for direct production of NO<sub>x</sub> is observed during this time in the Northern hemisphere, and the exact source-region of the NO<sub>x</sub> values is not clear from these observations. However, it should be pointed out that the NO<sub>x</sub> mixing ratios transported down into the stratosphere in January/February 2004 in the Northern hemisphere are nearly one order of magnitude larger than the amounts of NO<sub>x</sub> produced due to the solar event in October/November 2003, which was one of the largest solar events on record! Some short-lived increases of NO<sub>x</sub> are observed in the Southern hemisphere at altitudes above 60 km, most notably before the large solar event in mid-October 2003 and on November 22. These short-lived increases may be connected to energetic electron precipitation (e.g., due to the geomagnetic storms before and after the solar event, as also discussed in 16.5.1). However, it should be pointed out that the values observed are much smaller than during the solar event, and nearly two orders of magnitude smaller than values transported down from the upper mesosphere or lower thermosphere in the polar winter.

To summarize, there is an impact of energetic electron precipitation on the middle atmosphere down to the upper stratosphere. It clearly exceeds the impact of even very large solar events in some winters. However, it is to date not clear in which altitudes these very large NO<sub>x</sub> values are produced—either in the upper mesosphere or lower thermosphere; direct production due to energetic electron precipitation below ≈80 km altitude is small both compared to the direct impact of large solar events, and compared to the indirect contribution of NO<sub>x</sub> from the upper mesosphere and lower thermosphere.

**Acknowledgements** This work was funded within the framework of the priority program *Climate and Weather of the Sun-Earth System* CAWSES by the *Deutsche Forschungsgemeinschaft* as project *SI-1088/1-3*. The authors gratefully acknowledge the work of S. Kazeminejad, who is now at the *German Space Agency* DLR. M. Sinnhuber also gratefully acknowledges funding by the University of Bremen. MIPAS data were kindly provided by B. Funke, Instituto de Astrofísica de Andalucía, and G. Stiller, KIT. The authors would like to thank Bernd Funke for initiating and coordinating the Heppa intercomparison initiative, and U. Berger for providing the LIMA data.

## References

- Berger, U. (2008). Modeling of middle atmosphere dynamics with LIMA. *Journal of Atmospheric and Solar-Terrestrial Physics*, 70, 1170–1200.
- Boehringer, H., Fahey, D. W., Fehsenfeld, F. C., & Ferguson, E. E. (1983). The role of ion-molecule reactions in the conversion of N<sub>2</sub>O<sub>5</sub> to HNO<sub>3</sub> in the stratosphere. *Planetary and Space Science*, 31, 185–191. doi:10.1016/0032-0633(83)90053-3.
- Brasseur, G., & Chatel, A. (1983). Modelling of stratospheric ions: a first attempt. *Annales Geophysicae*, 1, 173–185.
- Callis, L. B., Natarajan, M., Lambeth, J. D., & Baker, D. N. (1998). Solar-atmospheric coupling by electrons (SOLACE) 2. Calculated stratospheric effects of precipitating electrons, 1979–1988. *Journal of Geophysical Research*, 103, 28421–28438.
- Chakrabarty, D. K., & Ganguly, S. (1989). On significant quantities of negative ions observed around the mesopause. *Journal of Atmospheric and Solar-Terrestrial Physics*, 51, 983–989.

- Chipperfield, M. (1999). Multiannual simulations with a three-dimensional chemical transport model. *Journal of Geophysical Research*, 104(D1), 1781–1805.
- Clilverd, M. A., Seppälä, A., Rodger, C. J., Mlynczak, M. G., & Kozyra, J. U. (2009). Additional stratospheric NO<sub>x</sub> production by relativistic electron precipitation during the 2004 spring NO<sub>x</sub> descent event. *Journal of Geophysical Research*, 114. doi:10.1029/2008JA013472.
- Crutzen, P. J., Isaksen, I. S., & Reid, G. C. (1975). Solar proton events: stratospheric sources of nitric oxide. *Science*, 189, 457–458.
- Dee, D. P., Uppala, S. M., Simmons, A. J., Berrisford, P., Poli, P., Kobayashi, S., Andrae, U., Balmaseda, M. A., Balsamo, G., Bauer, P., Bechtold, P., Beljaars, A. C. M., van de Berg, L., Bidlot, J., Bormann, N., Delsol, C., Dragani, R., Fuentes, M., Geer, A. J., Haimberger, L., Healy, S. B., Hersbach, H., Holm, E. V., Isaksen, L., Kallberg, P., Köhler, M., Matricardi, M., McNally, A. P., Monge-Sanz, B. M., Morcrette, J.-J., Park, B.-K., Peubey, C., de Rosnay, P., Tavolato, C., Thepaut, J.-N., & Vitart, F. (2011). The era-interim reanalysis: configuration and performance of the data assimilation system. *Quarterly Journal of the Royal Meteorological Society*, 137, 553–597.
- Fischer, H., Birk, M., Blom, C., Carli, B., Carlotti, M., von Clarmann, T., Delbouille, L., Dudhia, A., Ehhalt, D., Endemann, M., Flaud, J. M., Gessner, R., Kleinert, A., Koopmann, R., Langen, J., Lopez-Puertas, M., Mosner, P., Nett, H., Oelhaf, H., Perron, G., Remedios, J., Ridolfi, M., Stiller, G., & Zander, R. (2008). Mipas: an instrument for atmospheric and climate research. *Atmospheric Chemistry and Physics*, 8, 2151–2188.
- Fritzenwallner, J., & Kopp, E. (1998). Model calculations of the negative ion chemistry in the mesosphere with special emphasis on the chlorine species and the formation of cluster ions. *Advances in Space Research*, 21, 891–894.
- Funke, B., López-Puertas, M., Fischer, H., Stiller, G., von Clarmann, T., Wetzell, G., Carli, B., & Belotti, C. (2007). Comment on ‘Origin of the January–April 2004 increase in stratospheric NO<sub>2</sub> observed in northern polar latitudes’ by Jean-Baptiste Renard et al. *Geophysical Research Letters*, 34. doi:10.1029/2006GL027518.
- Funke, B., Baumgaertner, A. J. G., Calisto, M., Egorova, T., Jackman, C. H., Kieser, J., Krivolutsky, A., López-Puertas, M., Marsh, D. R., Reddmann, T., Rozanov, E., Salm, S.-M., Sinnhuber, M., Stiller, G., Verronen, P. T., Versick, S., von Clarmann, T., Vyushkova, T. Y., Wieters, N., & Wissing, J.-M. (2011). Composition changes after the “Halloween” solar proton event: the High-Energy Particle Precipitation in the Atmosphere (HEPPA) model versus MIPAS data inter-comparison study. *Atmospheric Chemistry and Physics*, 11, 9089–9139.
- Heaps, M. G. (1978). Parameterization of the cosmic ray ion-pair production rate above 18 km. *Planetary and Space Science*, 20, 513–517.
- Horne, R. B., Lam, M. M., & Green, J. C. (2009). Energetic electron precipitation from the outer radiation belt during geomagnetic storms. *Geophysical Research Letters*, 36. doi:10.1029/2009GL040236.
- Jackman, C., McPeters, R., Labow, G., Praderas, C., & Fleming, E. (2001). Northern hemisphere atmospheric effects due to the July 2000 solar proton events. *Geophysical Research Letters*, 28, 2883–2886.
- Jackman, C., DeLand, M., Labow, G., Fleming, E., Weisenstein, D., Ko, M., Sinnhuber, M., Anderson, J., & Russell, J. (2005a). Neutral atmospheric influences of the solar proton events in October–November 2003. *Journal of Geophysical Research*, 110, A09S27. doi:10.1029/2004JA01088.
- Jackman, C. H., DeLand, M. T., Labow, G. J., Fleming, E. L., Weisenstein, D. K., Ko, M. K. W., Sinnhuber, M., Anderson, J., & Russell, J. M. (2005b). The influence of the several very large solar proton events in years 2000–2003 on the neutral middle atmosphere. *Advances in Space Research*, 35, 445–450.
- Kazeminejad, S. (2009). *Analysis of the middle atmosphere’s response to energetic particle events*. Ph.D. thesis, University of Bremen.
- Kazil, J. (2002). *The University of Bern atmospheric ion model: time-dependent ion modeling in the stratosphere, mesosphere and lower thermosphere*. Ph.D. thesis, University of Bern.

- Kinnersley, J. S. (1996). The climatology of the stratospheric 'THIN AIR' model. *Quarterly Journal of the Royal Meteorological Society*, *122*(529, Part A), 219–252.
- Kopp, E. (1996). Electron and ion densities. In W. Dieminger, G. K. Hartman & R. Leitinger (Eds.), *The upper atmosphere, data analysis and interpretation* (pp. 620–630). Berlin: Springer.
- Kopp, E., & Fritzenwallner, J. (1997). Chlorine and bromine ions in the D-region. *Advances in Space Research*, *20*, 2111–2155.
- Lary, D. J. (1997). Catalytic destruction of stratospheric ozone. *Journal of Chemical Physics*, *102*, 21515–21526.
- López-Puertas, M., Funke, B., Gil-López, S., von Clarmann, T., Stiller, G. P., Höpfner, M., Kellmann, S., Fischer, H., & Jackman, C. H. (2005a). Observation of NO<sub>x</sub> enhancements and ozone depletion in the Northern and Southern Hemispheres after the October–November 2003 solar proton events. *Journal of Geophysical Research*, *110*, A09S43. doi:10.1029/2005JA01105.
- López-Puertas, M., Funke, B., Gil-López, S., von Clarmann, T., Stiller, G. P., Höpfner, M., Kellmann, S., Tsidu, G. M., Fischer, H., & Jackman, C. H. (2005b). HNO<sub>3</sub>, N<sub>2</sub>O<sub>5</sub>, and ClONO<sub>2</sub> enhancements after the October–November 2003 solar proton events. *Journal of Geophysical Research*, *110*, A09S44. doi:10.1029/2005JA011051.
- López-Puertas, M., Funke, B., von Clarmann, T., Fischer, H., & Stiller, G. P. (2006). The stratospheric and mesospheric NO<sub>y</sub> in the 2002–2004 polar winters as measured by MIPAS/ENVISAT. *Space Science Reviews*, *125*, 403–416. doi:10.1007/s11214-006-9073-2.
- Porter, H. S., Jackman, C. H., & Green, A. E. S. (1976). Efficiencies for production of atomic nitrogen and oxygen by relativistic proton impact in air. *Journal of Chemical Physics*, *65*, 154–167.
- Prather, M. J. (1986). Numerical advection by conservation of second-order moments. *Journal of Geophysical Research*, *91*(D6), 6671–6681.
- Ramarson, R. A. (1989). *Modélisation locale, à une et trois dimensions des processus photochimiques de l'atmosphère moyenne*. Ph.D. thesis, Université Paris VI.
- Randall, C. E., Siskind, D. E., & Bevilaqua, R. M. (2001). Stratospheric NO<sub>x</sub> enhancements in the southern hemisphere vortex in winter/spring of 2000. *Geophysical Research Letters*, *28*, 2385–2388.
- Rees, M. H. (1998). *Physics and chemistry of the upper atmosphere*. Cambridge: Cambridge University Press.
- Renard, J.-B., Blelly, P.-L., Bourgeois, Q., Chartier, M., Goutail, F., & Orsolini, Y. J. (2006). Origin of the January–April 2004 increase in stratospheric NO<sub>2</sub> observed in the northern polar latitudes. *Geophysical Research Letters*, *33*. doi:10.1029/2005GL025450.
- Rohen, G. J., von Savigny, C., Sinnhuber, M., Eichmann, K.-U., Llewellyn, E. J., Kaiser, J. W., Jackman, C. H., Kallenrode, M.-B., Schroeter, J., Bovensmann, H., & Burrows, J. P. (2005). Ozone depletion during the solar proton events of Oct./Nov. 2003 as seen by SCIAMACHY. *Journal of Geophysical Research*, *110*, A09S39.
- Rusch, D. W., Gerard, J.-C., Solomon, S., Crutzen, P. J., & Reid, G. C. (1981). The effect of particle precipitation events on the neutral and ion chemistry of the middle atmosphere, 1. Odd nitrogen. *Planetary and Space Science*, *29*, 767–774.
- Russell, J. M., Gordley, L. L., Park, J. H., Drayson, S. R., Hesketh, W. D., Cicerone, R. J., Tuck, A. F., Frederick, J. E., Harries, J. E., & Crutzen, P. J. (1993). The HaLogen Occultation Experiment. *Journal of Geophysical Research*, *98*, 10777–10797.
- Sander, S. P., Friedl, R. R., Ravishankara, A. R., Golden, D. M., Kolb, C. E., Kurylo, M. J., Molina, M. J., Moortgat, G. K., Keller-Rudek, H., Finlayson-Pitts, B. J., Wine, P., Huie, R. E., & Orkin, V. L. (2006). Chemical kinetics and photochemical data for use in atmospheric studies—evaluation number 15. *JPL Publication*, *06*(2).
- Shine, K. P. (1987). The middle atmosphere in the absence of dynamical heat fluxes. *Quarterly Journal of the Royal Meteorological Society*, *113*, 603–633.
- Simmons, A., Uppala, S., Dee, D., & Kobayashi, S. (2006). ERA-Interim: new ECMWF reanalysis products from 1989 onwards. *ECMWF Newsletter*, *110*. Winter 2006/2007.
- Sinnhuber, B.-M., Weber, M., Amankwah, A., & Burrows, J. P. (2003a). Total ozone during the unusual Antarctic winter of 2002. *Geophysical Research Letters*, *30*, 11. doi:10.1029/

2002GL016798.

- Sinnhuber, B.-M., von der Gathen, P., Sinnhuber, M., Rex, M., König-Langlo, G., & Oltmans, S. J. (2006). Large decadal scale changes of polar ozone suggest solar influence. *Atmospheric Chemistry and Physics*, 6, 1835–1841.
- Sinnhuber, M., Burrows, J. P., Künzi, K. F., Chipperfield, M. P., Jackman, C. H., Kallenrode, M.-B., & Quack, M. A. (2003b). A model study of the impact of magnetic field structure on atmospheric composition during solar proton events. *Geophysical Research Letters*, 30, L01818. doi:10.1029/2003GL017265.
- Sinnhuber, M., Jackman, C. H., & Kallenrode, M.-B. (2003c). The impact of large solar proton events on ozone in the polar stratosphere—a model study. In C. Zerefos (Ed.), *Proceedings quadrennial ozone symposium*, 1–8 June 2004, Kos, Greece.
- Sinnhuber, M., Kazeminejad, S., & Wissing, J. M. (2011). Interannual variation of NO<sub>x</sub> from the lower thermosphere to the upper stratosphere in the years 1991–2005. *Journal of Geophysical Research*, 116. doi:10.1029/2010JA015825.
- Siskind, D., Nedoluha, G., Randall, C., Fromm, M., & Russell III, J. M. (2000). An assessment of southern hemisphere stratospheric NO<sub>x</sub> enhancements due to transport from the upper atmosphere. *Geophysical Research Letters*, 27, 329–332.
- Siskind, D. E., & Russell III, J. M. (1996). Coupling between middle and upper atmospheric NO: constraints from HALOE observations. *Geophysical Research Letters*, 23, 137–140.
- Solomon, S., & Crutzen, P. J. (1981). Analysis of the August 1972 solar proton event including chlorine chemistry. *Journal of Geophysical Research*, 86, 1140–1146. doi:10.1029/JC086iC02p01140.
- Solomon, S., Rusch, D. W., Gerard, J.-C., Reid, G. C., & Crutzen, P. J. (1981). The effect of particle precipitation events on the neutral and ion chemistry of the middle atmosphere II: odd hydrogen. *Planetary and Space Science*, 29, 885–892.
- Solomon, S., Reid, G. C., Rusch, D. W., & Thomas, R. J. (1983). Mesospheric ozone depletion during the solar proton event of July 13, 1983, part II: comparison between theory and measurements. *Geophysical Research Letters*, 10, 257–260.
- Swider, W., & Keneshea, T. J. (1973). Decrease of ozone and atomic oxygen in the lower mesosphere during a PCT event. *Planetary and Space Science*, 21, 1969–1973.
- Verronen, P. T. (2006). *Ionosphere-atmosphere interaction during solar proton events*. Ph.D. thesis, University of Helsinki.
- Verronen, P. T., Funke, B., López-Puertas, M., Stiller, G. P., von Clarmann, T., Glatthor, N., Enell, C.-F., Turunen, E., & Tamminen, J. (2008). About the increase of HNO<sub>3</sub> in the stratopause region during the Halloween 2003 solar proton event. *Geophysical Research Letters*, 35, L20809. doi:10.1029/2008GL035312.
- Verronen, P. T., Rodger, C. J., Clilverd, M. A., & Wang, S. (2011). First evidence of mesospheric hydroxyl response to electron precipitation from the radiation belts. *Journal of Geophysical Research*, 116, D07307. doi:10.1029/2010JD014965.
- Viggiano, A. A., Morris, R. A., & Doren, J. M. V. (1994). Ion chemistry of ClONO<sub>2</sub> involving NO<sub>3</sub><sup>-</sup> core ions: a detection scheme for ClONO<sub>2</sub> in the atmosphere. *Journal of Geophysical Research*, 99, 8221–8224.
- von Clarmann, T., Glatthor, N., Höpfner, M., Kellmann, S., Ruhnke, R., Stiller, G. P., Fischer, H., Funke, H., Gil-López, S., & López-Puertas, M. (2005). Experimental evidence of perturbed odd hydrogen and chlorine chemistry after the October 2003 solar proton events. *Journal of Geophysical Research*, 110, A09S45. doi:10.1029/2005JA011053.
- Winkler, H. (2007). *Response of middle atmospheric ozone to solar proton events in a changing geomagnetic field*. Ph.D. thesis, University of Bremen.
- Winkler, H., Sinnhuber, M., Notholt, J., Kallenrode, M.-B., Steinhilber, F., Vogt, J., Zieger, B., Glassmeier, K.-H., & Stadelmann, A. (2008). Modelling impacts of geomagnetic field variations on middle atmospheric ozone responses to solar proton events on long time scales. *Journal of Geophysical Research*, 113, D02302. doi:10.1029/2007JD008574.
- Winkler, H., Kazeminejad, S., Sinnhuber, M., Kallenrode, M.-B., & Notholt, J. (2009). The conversion of mesospheric HCl into active chlorine during the solar proton event in July 2000



- in the northern polar region. *Journal of Geophysical Research*, 114, D00I03. doi:[10.1029/2008JD011587](https://doi.org/10.1029/2008JD011587).
- Winkler, H., Kazeminejad, S., Sinnhuber, M., Kallenrode, M.-B., & Notholt, J. (2011). Correction to “Conversion of mesospheric HCl into active chlorine during the solar proton event in July 2000 in the northern polar region”. *Journal of Geophysical Research*, 116, D17303. doi:[10.1029/2011JD016274](https://doi.org/10.1029/2011JD016274).
- Wissing, J.-M., & Kallenrode, M.-B. (2009). Atmospheric Ionisation Module Osnabrück (AIMOS): A 3-D model to determine atmospheric ionization by energetic charged particles from different populations. *Journal of Geophysical Research*, 114, A06104. doi:[10.1029/2008JA013884](https://doi.org/10.1029/2008JA013884).
- Wissing, J.-M., Kallenrode, M.-B., Wieters, N., Winkler, H., & Sinnhuber, M. (2010). Atmospheric Ionisation Module Osnabrück (AIMOS) 2: Total particle inventory in the October / November 2003 event and ozone. *Journal of Geophysical Research*, 115, A02308. doi:[10.1029/2009JA014419](https://doi.org/10.1029/2009JA014419).
- Zipf, E. C., Espy, P. J., & Boyle, C. F. (1980). The excitation and collisional deactivation of metastable N(2P) atoms in auroras. *Journal of Geophysical Research*, 85, 687–694.